Graphene-coated holey metal films: tunable molecular sensing by surface plasmon resonance

Nicolas Reckinger,[1,†] Alexandru Vlad,[2,†] Sorin Melinte,[2] Jean-François Colomer,[1] Michaël Sarrazin[1,†*]

[1]*Research Center in Physics of Matter and Radiation (PMR), Department of Physics,*
University of Namur, 61 rue de Bruxelles, B-5000 Namur, Belgium
[2]*Institute of Information, Communication Technologies,*
Electronics and Applied Mathematics, Electrical Engineering,
Universite catholique de Louvain, Louvain-la-Neuve, B-1348, Belgium and
[†]*These authors contributed equally to this work*

We report on the enhancement of surface plasmon resonances in a holey bidimensional grating of subwavelength size, drilled in a gold thin film coated by a graphene sheet. The enhancement originates from the coupling between charge carriers in graphene and gold surface plasmons. The main plasmon resonance peak is located around 1.5 μm. A lower constraint on the gold-induced doping concentration of graphene is specified and the interest of this architecture for molecular sensing is also highlighted.
[†]*These authors contributed equally to this work.*

Plasmonic devices offer valuable platforms for a wide range of emerging molecular detection schemes. Among such applications, biosensors are very promising especially from the point of view of lab-on-a-chip (LOC) technologies.[1] Indeed, plasmon resonances are characterized by both a strong electric field and a great sensitivity to environmental conditions. As a consequence, adsorbed species can be detected through the resonance wavelength shift. In addition, the strong electric field enhancement allows for surface enhanced Raman spectroscopy, which can be used for single molecule detection.[2]

Surface plasmons (SPs) require specific conditions to be excited. For instance, in the Kretschmann configuration, a light beam is totally internally reflected in a prism on which a metallic film is deposited and triggers the generation of SPs.[3] In a holey metal film, SPs can be excited by a normal incidence light beam.[4] Light is scattered due to the corrugations and the evanescent diffraction orders can excite SPs.[5] For a metallic layer accommodating an array of holes with subwavelength size, it is possible to probe SPs by simply measuring the intensity of the transmitted light. Such a simple configuration is much more practical in the LOC context and it has been widely studied since the pioneering work of Ebbesen *et al.* in 1998.[4]

Recent theoretical works have shown that doping can induce SP modes in graphene.[6–8] Graphene, which appears as a monoatomic layer made of sp[2] carbon atoms in a hexagonal lattice configuration, presents a plethora of amazing properties.[9] In that context, SPs have been observed for graphene doped by charge transfer from metal thin films,[10–13] external atoms[14] or electrostatic gating[15,16]. It has been also suggested that SPs could be excited in graphene on a periodically structured
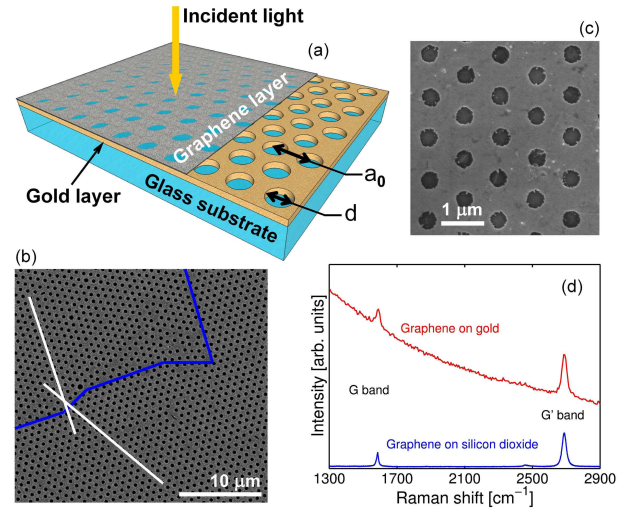

FIG. 1: (Color online). (a) Sketch of the device. A microscope glass slide with a thickness of 1 mm is coated with a 25-nm-thick gold film. The metallic film is perforated by a hexagonal array of holes with a grating parameter $a_0 = 980$ nm. The hole diameter is $d = 405$ nm. The perforated gold film is coated by a graphene sheet. (b) Scanning electron microscopy (SEM) picture of two domains (delimited by blue lines) with different orientations (white straight lines) in the holey gold film. (c) SEM top view of the final device. (d) Raman spectroscopy of the synthesized graphene layer, transferred on gold and on silicon dioxide.

substrate[17,18] or via regular patterns in graphene.[19–25] A recent experimental result showed that graphene SPs can be excited in a Kretschmann configuration using graphene deposited on a planar gold layer.[10] A different approach[26] was used in which SP resonance tunability was achieved by electromagnetic field coupling between a graphene sheet and SPs excited in gold nanoparticles.

In the present work, we describe and study an opti-
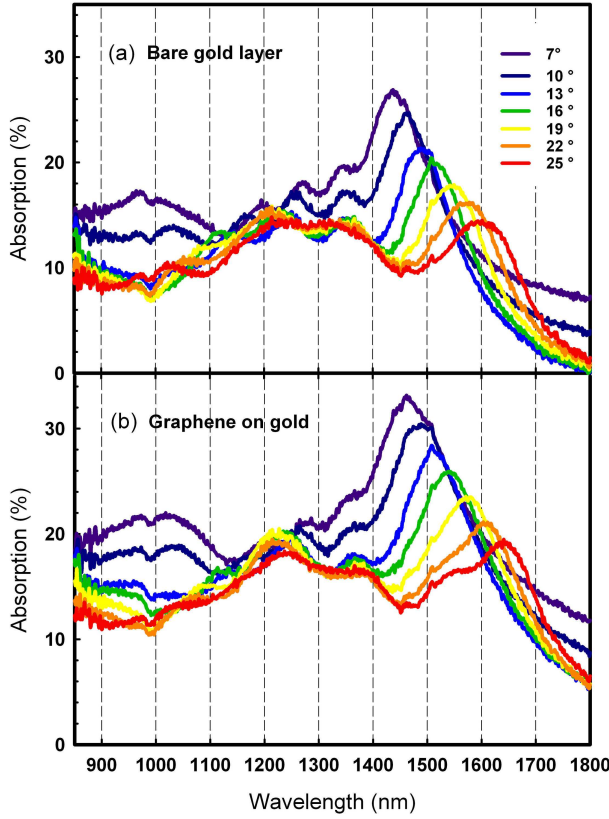
*e-mail: michael.sarrazin@unamur.be

FIG. 2: (Color online). Optical characteristics of the device. Absorption spectra of the uncoated holey gold film (a) and of the graphene-coated device (b) for various incidence angles.

cal device constituted by a planar hexagonal array of subwavelength-sized holes in a gold thin film functionalized with a graphene layer. The entire device is built on a glass substrate. Resonances of the device are measured for various incidence angles. It is shown that graphene enhances the plasmon resonances and induces a redshift of the resonance wavelength. This plasmonic device used as a molecular sensor displays a wavelength shift which is highly sensitive to environmental conditions.

Figure 1(a) gives a conceptual illustration of the nanostructured plasmonic platform. It was fabricated by using colloidal nanosphere lithography. Briefly, polystyrene spheres (980 nm in diameter, Microparticles GmbH) were deposited on soda-lime glass plates via an interfacial self-assembly protocol.[27,28] Reactive ion etching using O_2 chemistry (Oxford Plasmalab, 100 W RF power, 100 sccm O_2, 25 mTorr, 12 min) was used to reduce the size of the colloids to half the nominal diameter. Subsequently, 2 nm of Ti followed by 25 nm of Au were deposited using physical vapor deposition. The liftoff was performed using adhesive tape and ultrasonication in dichloromethane. Figure 1(b) shows a Scanning Electron Microscopy (SEM) top view of the array made of large periodic crystal-like domains.

Graphene was synthesized by atmospheric pressure chemical vapor deposition at 1000 °C on copper foils with

methane as carbon source.[29–31] The copper foil was inserted into a quartz reactor inside a hot-wall furnace. After annealing at 1000 °C for 30 min under argon (500 ml/min) and hydrogen (100 ml/min), methane was admitted (0.5 ml/min) for 15 min to grow graphene. It was next cooled down rapidly under argon and hydrogen. After spin-coating a polymethyl methacrylate (PMMA) film over graphene,[32] the copper foil was etched in aqueous ammonium persulfate. Next, the PMMA/graphene stack was rinsed in distilled water and transferred onto the holey gold/glass substrate. The PMMA film was then removed by soaking into acetone and finally blown dry with nitrogen. Figure 1(c) shows a SEM top view of the resulting device. In addition, a reference sample with graphene over planar gold was fabricated. Graphene was also transferred on silicon dioxide (300-nm-thick) for Raman inspection. The detection of G ($\sim$1590 cm^{-1}) and G$'$ ($\sim$2690 cm^{-1}) bands testifies of the presence of graphene (see the Raman spectra in Fig. 1(d), for graphene over planar gold and silicon dioxide). No disorder-related D band ($\sim$1350 cm^{-1}) is observed, suggestive of virtually defect-free graphene.

Optical characterization was carried out at various incidence angles by using an integrating sphere setup mounted on a Perkin-Elmer Lambda 750S UV/Vis/NIR spectrophotometer. The sample was positioned such that the light source faces the graphene surface at normal incidence. Figure 2(a) shows the absorption (A_B) of the bare holey gold film (i.e. without graphene). The extinction of the graphene-coated holey gold film is shown in Fig. 2(b) (A_G). The typical absorption peaks denote surface plasmon polaritons.[5] As it can be observed, graphene induces a redshift of the plasmon resonance peaks and dramatically enhances the absorption of the device up to 40% (see also Fig. 3(a)). It is noteworthy that the main plasmon resonance peak is located around 1.5 μm, close to the wavelength range of interest to optoelectronic applications.

The relative absorption R, calculated as $R = (A_G - A_B)/A_B$, is shown in Fig. 3(a). The role of SPs is anticipated from the relative shift of the peaks in Fig. 3(a) for the considered incidence angles. In addition, the relative absorption of a graphene layer deposited on unstructured gold (black curve in Fig. 3(a)) shows a weak enhancement by contrast with the corrugated gold film. Since corrugated metallic films allow for SP modes, it is a strong argument for the coupling between SPs on gold and graphene. To further support this, we have run numerical simulations based on a homemade code which rests on a rigorous coupled wave analysis (RCWA) method.[5] By considering the frequency − and position − dependence of the electric field $\mathbf{E}(\omega, \mathbf{r})$ inside a given material, the absorbed power is given by:[33]

$$P_{abs} = -\frac{\varepsilon_0 \omega}{2} \int_V \varepsilon''(\omega, \mathbf{r}) |\mathbf{E}(\omega, \mathbf{r})|^2 \, d^3 r \qquad (1)$$

where ε_0 is the vacuum permittivity, ε'' is the imaginary
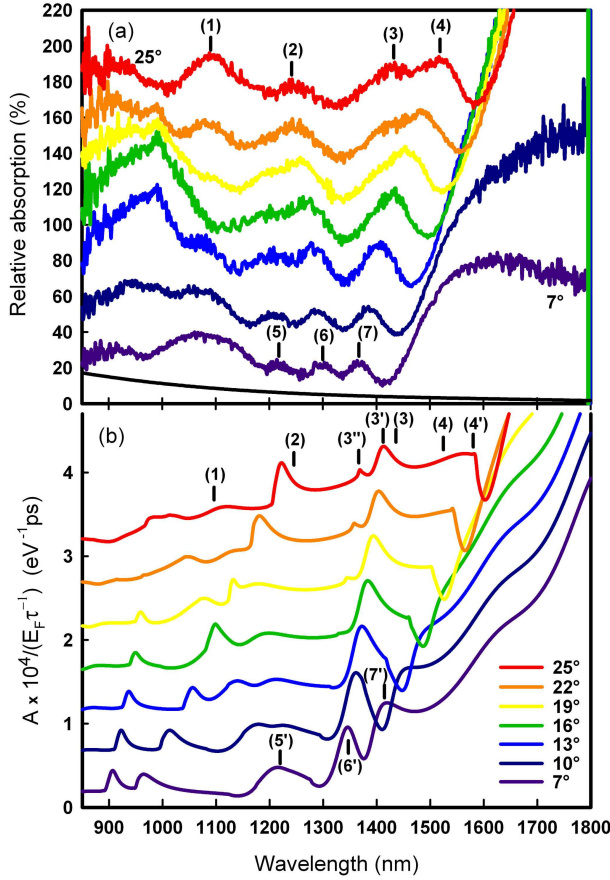
FIG. 3: (Color online). (a) Relative absorption of the graphene-coated versus uncoated gold for various incidence angles. The black curve represents the relative absorption for a non structured metal film. For the sake of clarity, each curve is shifted vertically by 25 units with respect to the previous one. (b) Numerical simulation of the absorption of the graphene-coated device for various angles of incidence. For the sake of clarity, each curve is shifted vertically by 0.5 units with respect to the previous one.

part of the relative permittivity of the medium (here the graphene layer), and V its volume. This formula can be expressed according to the real part of the medium conductivity, i.e. $\gamma' = \varepsilon_0 \omega \varepsilon''$. For a two-dimensional-like medium, such as graphene, we get

$$P_{\text{abs}} = -\frac{1}{2} \int_S \gamma'(\omega, \rho) \left| \mathbf{E}(\omega, \rho) \right|^2 \mathrm{d}^2 \rho \qquad (2)$$

with S the surface, ρ the position vector along the graphene layer, and where γ' is the real part of the graphene conductivity.[34,35] γ' can be restricted to the intraband term:[7,35,36]

$$\gamma' = \frac{e^2 E_{\text{F}}}{\pi \hbar^2} \frac{\tau^{-1}}{(\omega^2 + \tau^{-2})} \qquad (3)$$

with $\hbar$ the reduced Planck constant, e the electron charge, E_{F} the Fermi level, and τ the relaxation time.
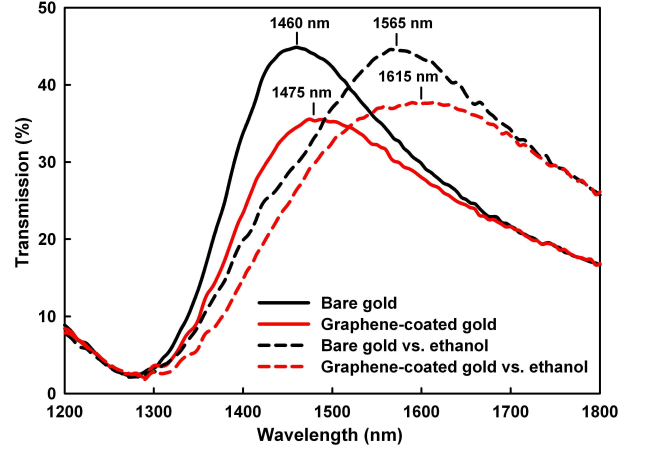

FIG. 4: (Color online). Zeroth order transmission through graphene-coated gold (red curves) and bare gold (black curves) devices. A significant peak shift occurs when ethanol is deposited on the devices (dashed curves) by contrast with cases without ethanol (solid curves). Compared to the bare gold device, for the device coated with graphene, the wavelength-shift is enhanced by 33%. Peaks retrieve their initial positions after few minutes when ethanol is fully evaporated.

The intraband approximation is legitimate since no resonance occurs below 900 nm, suggesting that $E_{\text{F}} \geq 0.7$ eV,[19,36] corresponding to a charge density $n \geq 4 \times 10^{13}$ cm^{-2}.[7] Albeit large, these values are in agreement with those achieved in other works.[11,12,14]

Let us now consider $\mathbf{E}(\omega, \mathbf{r})$ as the electric field of the electromagnetic wave scattered at the air/gold interface without graphene. We suppose that such an electromagnetic field is not significantly modified by the graphene layer as a first approximation. In addition, we suppose that the extrinsic conductivity of graphene due to the gold film can be considered as uniform, i.e. γ' does not depend on ρ. The incident power is given by $P_{\text{in}} = (1/2)\sigma c \varepsilon_0 E_{\text{in}}^2$, where c is the speed of light, σ is the area of the unit cell of the array, and E_{in} the electric field amplitude of the incident wave. Then, the absorption of graphene is defined as $A = |P_{\text{abs}}| / P_{\text{in}}$, and assuming that we work at frequencies $\omega \gg \tau^{-1}$, we get

$$A = K_0 \lambda^2 \frac{1}{E_{\text{in}}^2} \frac{1}{\sigma} \int_S \left| \mathbf{E}(\lambda, \rho) \right|^2 d^2 \rho \qquad (4)$$

where λ is the wavelength ($\lambda = 2\pi c/\omega$) and $K_0 = e^2 E_{\text{F}} \tau^{-1}/(4\pi^3 c^3 \varepsilon_0 \hbar^2)$. Except for K_0, which is a mere factor of proportionality, A can be easily computed numerically using our homemade RCWA code, allowing to propagate the electromagnetic field on a bare perforated gold layer on glass. The permittivities of materials are taken from the literature.[37] In Fig. 3(b), we display the calculated quantity $A/E_{\text{F}} \tau^{-1}$ for different incidence angles. Markers (noted as numerals, from (1) to (7), from (3') to (7'), and (3'')) have been added in Figs. 3(a) and 3(b) for comparison. The global pattern in Fig. 3(b)

matches very well the experimental data shown in Fig. 3(a). This supports the supposition that the enhancement is due to graphene conductivity coupled with surface modes, i.e. SPs at the gold/air interface. We note a few discrepancies, for instance, the peak at wavelength (3) seems to result from two shifted resonances at wavelengths (3′) and (3″). Peaks at wavelengths (5) to (7) also appear shifted to wavelengths (5′) to (7′). These differences between experiment and numerical simulations are due to the fact that we consider a perfectly periodic hole array in our simulation while the real one is constituted of a set of many crystal-like domains (see the SEM picture in Fig. 1(b)). In addition, the retroactive role of the graphene layer on the electric field $\mathbf{E}(\omega, \mathbf{r})$ is not considered. The present theoretical results indicate that graphene must be doped in order to support SPs (here, the doping is extrinsic and provided by the gold layer). Indeed, if $K_0 = 0$ (i.e. absence of doping) there is no absorption. In addition, the intraband approximation is also supported by the fact that the interband term[35,36] is unable to reproduce the experimental patterns shown in Fig. 3(a).

In the following, we show that graphene-coated holey gold films enhance the wavelength shift against the environment changes proving the versatility of this configuration for LOC sensing applications. We have analyzed the response of the devices in the presence of ethanol at the main plasmon resonance around 1.5 μm. Ethanol is first spread on the graphene side of the device. To avoid thin film interferences due to a thick ethanol layer, a delay of 30 seconds is set to allow ethanol to partially evaporate. This preserves an adsorbed layer with a subwavelength thickness. Transmission is then recorded. Figure 4 displays the response of the devices when in presence of ethanol. The zeroth order transmissions at normal incidence are plotted where a typical peak is observed for wavelengths around a SP resonance.[5] The transmission peak for both types of gold samples (graphene-coated and bare) is redshifted when exposed to ethanol. However, the graphene-coated sample shows a higher wavelength-shift sensitivity − the resonance peak shift being 33% greater than for the bare device. After complete evaporation of ethanol, the peaks retrieve their initial position.

Note that the wavelength shift as well as the transmission decrease (i.e. the absorption enhancement) are related. Indeed, the surface plasmon wave vector $k_{\rm sp}$ must verify $k_{\rm sp} = |\mathbf{k}_{//} + \mathbf{g}|$, where $\mathbf{k}_{//}$ is the parallel component of the wave vector of the incident light wave with respect to the interface, and $\mathbf{g}$ is a vector of the reciprocal lattice. For the smallest non trivial vector $\mathbf{g}$ and for normal incidence, the wavelength $\lambda_{\rm sp}$ for which a plasmon resonance occurs can be roughly approximated by:[3,33]

$$\lambda_{\rm sp} \approx \frac{a_0\sqrt{3}}{2}Re\left\{\sqrt{\varepsilon_d + i\frac{\gamma'_d}{\omega\varepsilon_0}}\right\} \qquad (5)$$

where ε_d is the permittivity of the dielectric environment which surrounds the metallic layer and γ'_d the conductivity of the dielectric, which depends on the graphene layer conductivity. If γ' increases, the optical absorption increases (since $\gamma' = \varepsilon_0\omega\varepsilon''$), but $\lambda_{\rm sp}$ is also shifted. Moreover, the ethanol layer present on the device alters the combined permittivity ε_d and also causes shift and intensity changes.

In summary, nanostructured hybrid graphene-gold architectures enhance the wavelength shift in plasmonic sensors. The simple graphene-coated metal grating device allows for a facile optical characterization at normal incidence, without the need of a complex Kretschmann configuration, greatly improving the portability of the measurement setup. Moreover, the rich graphene surface chemistry offers unique functionalization protocols, enlarging further the sensor's versatility.[38]

[1] H. Craighead, Nature **442**, 387 (2006).
[2] M. Moskovits, Rev. Mod. Phys. **57**, 783 (1985).
[3] H. Raether, *Surface Plasmons on Smooth and Rough Surfaces and on Gratings* (Springer-Verlag, Berlin and Heidelberg, 1988).
[4] T. W. Ebbesen, H. J. Lezec, H. F. Ghaemi, T. Thio, and P. A. Wolff, Nature **391**, 667 (1998).
[5] M. Sarrazin, J.-P. Vigneron, and J.-M. Vigoureux, Phys. Rev. B **67**, 085415 (2003).
[6] S. H. Abedinpour, G. Vignale, A. Principi, M. Polini, W.-K. Tse, and A. H. MacDonald, Phys. Rev. B **84**, 045429 (2011).
[7] M. Jablan, H. Buljan, and M. Soljacic, Phys. Rev. B **80**, 245435 (2009).
[8] F. H. L. Koppens, D. E. Chang, and F. J. Garcia de Abajo, Nano Lett. **11**, 3370 (2011).
[9] A. K. Geim and K. S. Novoselov, Nature Mater. **6**, 183 (2007).
[10] O. Salihoglu, S. Balci, and C. Kocabas, Appl. Phys. Lett. **100**, 213110 (2012).
[11] P. A. Khomyakov, G. Giovannetti, P. C. Rusu, G. Brocks, J. van den Brink, and P. J. Kelly, Phys. Rev. B **79**, 195425 (2009).
[12] G. Giovannetti, P. A. Khomyakov, G. Brocks, V. M.

Karpan, J. van den Brink, and P. J. Kelly, Phys. Rev. Lett. **101**, 026803 (2008).

[13] Z. Fang, Y. Wang, Z. Liu, A. Schlather, P. M. Ajayan, F. H. L. Koppens, P. Nordlander, and N. J. Halas, ACS Nano **6**, 10222 (2012).

[14] S. Y. Shin, N. D. Kim, J. G. Kim, K. S. Kim, D. Y. Noh, Kwang S. Kim, and J. W. Chung, Appl. Phys. Lett. **99**, 082110 (2011).

[15] J. Chen, M. Badioli, P. Alonso-Gonzalez, S. Thongrattanasiri, F. Huth, J. Osmond, M. Spasenovic, A. Centeno, A. Pesquera, P. Godignon, *et al.*, Nature **487**, 77 (2012).

[16] Z. Fei, A. S. Rodin, G. O. Andreev, W. Bao, A. S. McLeod, M. Wagner, L. M. Zhang, Z. Zhao, M. Thiemens, G. Dominguez, *et al.*, Nature **487**, 82 (2012).

[17] X. Zhu, W. Yan, P. U. Jepsen, O. Hansen, N. A. Mortensen, and S. Xiao, Appl. Phys. Lett. **102**, 131101 (2013).

[18] A. Ferreira and N. M. R. Peres, Phys. Rev. B **86**, 205401 (2012).

[19] Yu. V. Bludov, A. Ferreira, N. M. R. Peres, and M. I. Vasilevskiy, Int. J. Mod. Phys. B **27** 1341001 (2013).

[20] A. Yu. Nikitin, F. Guinea, F. J. Garcia-Vidal, and L. Martin-Moreno, Phys. Rev. B **84**, 161407(R) (2011).

[21] A. Yu. Nikitin, F. Guinea, F. J. Garcia-Vidal, and L. Martin-Moreno, Phys. Rev. B **85**, 081405(R) (2012).

[22] A. Yu. Nikitin, F. Guinea, and L. Martin-Moreno, Appl. Phys. Lett. **101**, 151119 (2012).

[23] V. V. Popov, T. Yu. Bagaeva, T. Otsuji, and V. Ryzhii, Phys. Rev. B **81**, 073404 (2010).

[24] V. V. Popov, O. V. Polischuk, A. R. Davoyan, V. Ryzhii, T. Otsuji, and M. S. Shur, Phys. Rev. B **86**, 195437 (2012).

[25] S. Thongrattanasiri, F. H. L. Koppens, and F. J. Garcia de Abajo, Phys. Rev. Lett. **108**, 047401 (2012).

[26] J. Niu, Y. J. Shin, Y. Lee, J.-H. Ahn, and H. Yang, Appl. Phys. Lett. **100**, 061116 (2012).

[27] A. Vlad, A. Frölich, T. Zebrowski, C. A. Duţu, K. Busch, S. Melinte, M. Wegener, and I. Huynen, Adv. Funct. Mater. **23**, 1164 (2013).

[28] A. Vlad, I. Huynen, and S. Melinte, Nanotechnology **23**, 285708 (2012).

[29] X. Li, W. Cai, J. An, S. Kim, J. Nah, D. Yang, R. Piner, A. Velamakanni, I. Jung, E. Tutuc, *et al.*, Science **324**, 1312 (2009).

[30] B. Wu, D. Geng, Y. Guo, L. Huang, Y. Xue, J. Zheng, J. Chen, G. Yu, Y. Liu, L. Jiang, and W. Hu, Adv. Mater. **23**, 3522 (2011).

[31] N. Reckinger, A. Felten, C. N. Santos, B. Hackens, and J.-F. Colomer, arXiv:1303.3951 [cond-mat.mtrl-sci].

[32] A. Reina, X. Jia, J. Ho, D. Nezich, H. Son, V. Bulovic, M. S. Dresselhaus, and J. Kong, Nano Lett. **9**, 30 (2009).

[33] J. D. Jackson, *Classical Electrodynamics* (Wiley, 1998).

[34] N. W. Ashcroft and N. D. Mermin, *Solid State Physics* (Saunders, Philadelphia, PA, 1976).

[35] G. W. Hanson, J. Appl. Phys. **104**, 084314 (2008).

[36] G. W. Hanson, J. Appl. Phys. **103**, 064302 (2008).

[37] E. D. Palik, *Handbook of Optical Constants of Solids* (Academic, Boston, 1985).

[38] W. Gao, L. B. Alemany, L. Ci, and P. M. Ajayan, Nature Chem. **1**, 403 (2009).